Aldosterone acts via an ATP autocrine/paracrine system: The Edelman ATP hypothesis revisited

Julia Gorelik*†, Yanjun Zhang†‡, Daniel Sánchez‡, Andrew Shevchuk‡, Gregory Frolenkov§, Max Lab‡, David Klenerman¶, Christopher Edwards‖**, and Yuri Korchev‡***

‡Division of Medicine, Imperial College London, Medical Research Council Clinical Sciences Centre, London W12 0NN, United Kingdom; *National Heart and Lung Institute, Imperial College London, London SW3 6LY, United Kingdom; §Department of Physiology, University of Kentucky, Chandler Medical Center, Lexington, KY 40536; ¶Department of Chemistry, Cambridge University, Cambridge CB2 1EW, United Kingdom; and ‖Office of the Vice Chancellor, University of Newcastle upon Tyne, Newcastle upon Tyne NE1 7RU, United Kingdom

Communicated by Maria Iandolo New, Weill Medical College of Cornell University, New York, NY, August 22, 2005 (received for review July 19, 2005)

Aldosterone, the most important sodium-retaining hormone, was first characterized >50 years ago. However, despite numerous studies including the classical work of Isidore S. ''Izzy'' Edelman showing that aldosterone action depended on ATP production, the mechanism by which it activates sodium reabsorption via the epithelial sodium channel remains unclear. Here, we report experiments that suggest that one of the key steps in aldosterone action is via an autocrine/paracrine system. The hormone stimulates ATP release from the basolateral side of the target kidney cell. Prevention of ATP accumulation or its removal blocks aldosterone action. ATP then acts via a purinergic mechanism to produce contraction of small groups of adjacent epithelial cells. Patch clamping demonstrates that it is these contracted cells that have channel activity. With progressive recruitment of contracting cells, there is then a parallel increase in transepithelial electrical conductance. In common with other stimuli of sodium transport, this pathway involves phosphatidylinositol 3-kinase. Inhibition of phosphatidylinositol 3-kinase blocks both cell contraction and conductance. We put forward the hypothesis that redistribution of the cell volume caused by the lateral contraction results in apical swelling and that this change, in turn, disrupts the epithelial sodium channel interaction with the F-actin cytoskeleton, opening the channel and hence increasing sodium transport.

scanning ion conductance microscopy | scanning probe microscopy | epithelial sodium channel | renal epithelium

The sodium homeostasis regulatory hormone aldosterone was first identified in 1953 (1). Early studies on the biochemical mechanism of its action were reviewed by Edelman and Fimognari (2). This work was greatly helped by the introduction by Ussing and Zerahn (3) of the short-circuit current method for measuring sodium transport. Jean Crabbé (4, 5) first demonstrated the effect of aldosterone on sodium transport across toad bladder and skin and drew attention to the latent period of 60–90 min in the action of aldosterone. He postulated the synthesis or activation of an intermediate by aldosterone. Work by Edelman *et al*. (6) showed that inhibition of DNA-dependent RNA synthesis and of protein synthesis blocked the aldosterone effect. Edelman *et al*. (6) went on to demonstrate that aldosterone activation of sodium transport was critically dependent on ATP production. In substrate-depleted toad bladders, aldosterone had little or no effect, but the response was restored by adding glucose or pyruvate to the medium. Edelman suggested that a possible explanation of this absolute dependence on substrate was that, in the energy-depleted system, the rate of activation of sodium transport was limited by the local concentration of ATP. However, he felt that this hypothesis was questionable given that substrate-depleted toad bladders responded to vasopressin and to amphotericin B with a normal increase in sodium transport. This work became known as the ATP generation hypothesis of aldosterone action with ATP *inter alia* increasing the amount of energy available for the sodium pump.

In addition to hormonal stimulation (aldosterone, vasopressin, insulin), other factors are known to increase epithelial sodium transport, including hypotonic and mechanical stimulation (7). In recent work, Jans *et al*. (8) have shown that hypotonic treatment of renal epithelia induces a transient increase in intracellular Ca^{2+} through a mechanism that is sensitive to the purinergic P2 receptor antagonist suramin applied to the basolateral border only. They demonstrated that ATP was released from the cell and then acted via an autocrine/paracrine system to produce the suramin-sensitive rise of intracellular Ca^{2+}. These results are in keeping with a well described mechanism in which ATP is excreted from the cell and has a signaling function via an autocrine or paracrine system that acts through purinergic receptors of the P2 family (9). Taking these studies together, we formulated the hypothesis that aldosterone action might involve the stimulation and extracellular release of ATP, and that this might then have an autocrine/paracrine effect leading to an increase in sodium transport. Because one of the effects of hypotonic treatment is swelling of the cell and, bearing in mind the mechanical sensitivity of the sodium channel (10), we decided to study the morphological changes occurring during aldosterone stimulation and how they related to sodium transport. For this purpose, we have used scanning ion conductance microscopy (SICM), a well developed noninvasive live cell imaging technique (11, 12) in combination with patch-clamping (13, 14) that enables us to study not only the topographical changes of the cell apical membrane but also to relate them to ion channel activity.

Methods

Cell Culture. The experiments used a single A6 cell line (kindly provided by P. DeSmet, Katholieke Universiteit, Leuven, Belgium) carried out between 127–134 passages. Cells were cultured on membrane filters as described (11, 15).

The Scanning Ion Conductance Microscope (SICM) Set-Up. This method has been described (12, 16). Briefly, the sensitive SICM probe consists of a glass nanopipette filled with electrolyte (Fig. 1*A*). An Ag/AgCl electrode plugged into it is connected to a current amplifier that measures the ion current passing through the pipette tip. The probe, mounted on a three-axis piezo translation stage is modulated vertically 100 nm at 200 Hz when close to the sample surface. The modulated current is amplified and fed into a lock-in amplifier tuned to the modulation frequency. The output is connected to a DSP card to generate a feedback signal to maintain constant probe-sample separation

Abbreviations: SICM, scanning ion conductance microscopy; PI3K, phosphatidylinositol 3-kinase; G_t, transepithelial electrical conductance.

†J.G. and Y.Z. contributed equally to this work.

**To whom correspondence may be addressed. E-mail: y.korchev@ic.ac.uk or c.edwards@ncl.ac.uk.

www.pnas.org/cgi/doi/10.1073/pnas.0507008102

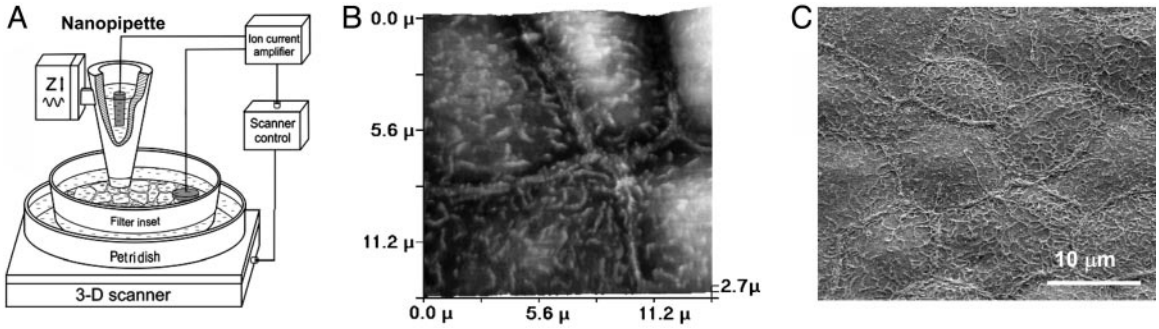

Fig. 1. Imaging of renal epithelial A6 cells. (*A*) Schematic diagram of SICM set-up. The A6 monolayer grown on a membrane filter insert is mounted on a 3D Piezo scanner controlled by a feedback and scan control system. The modulated glass nanopipette scans the apical side of the monolayer and obtains topographical images of the cell membrane. (*B*) SICM image of living A6 cells cultured on a membrane filter insert. (*C*) SEM image of a fixed A6 cell monolayer cultured on a membrane filter.

distance (≈40 nm) by moving the translation stage on which the sample is mounted in the vertical direction. The control/data acquisition electronics records both the lateral and vertical positions of the probe during the raster scanning and generates the topographical image.

Smart Patch Technique. The SICM set-up was also adapted for patch clamping (14). After obtaining the topographic images, the system positions the same nanopipette (now used as a patch pipette) precisely over an area or point of interest for patch recording. The feedback control is switched off, the pipette is lowered, and suction is applied to form a GΩ-seal. Ion channel recording is then performed by conventional patch clamp method in the cell-attach configuration.

L-15 medium (GIBCO, Paisley, U.K.) was used as the bath and pipette backfill solution for the SICM and patch clamp recordings. The micropipette when backfilled with L15 medium had an average tip resistance of 150 MΩ. For patch clamp recording, currents were sampled at 10 kHz and filtered at 2 kHz (–3 dB, 4-pole Bessel) by using an Axopatch 200B amplifier and PCLAMP 8.2 (Axon Instruments, Union City, CA), which was also used to generate the pulse protocols and analyze the single channel activity. A total of 60 patches were performed, equally probing three different types of the cells, contracted (in a total of 15 patches) and noncontracted (in a total of 45 patches) after acute stimulation by aldosterone.

Aldosterone Stimulation. A modified Kemendy protocol (15) tested the effects of aldosterone. Briefly, the mature A6 cell monolayer was maintained in the growth medium together with 10% FCS as above, but supplemented with 1.5 μM aldosterone (Sigma). After 24 h, the monolayer was incubated in a serum-free medium in the presence of aldosterone for another 24 h. The cells were then grown in serum- and aldosterone-free culture medium and incubated in a humidified incubator with 1% CO_2 in air for a further 48 h. During the experiments assessing aldosterone action, 1.5 μM aldosterone was re-added to both sides of the monolayer (15).

Hypotonic Stress. Before being used in the experiment, a well developed cell monolayer was bathed with an L-15 medium at room temperature, and then, to examine the effects of hypotonicity, A6 cells were exposed to basolateral 33.3% hypotonic stress by the addition of two parts L-15 medium and one part of distilled water.

To study the role of phosphatidylinositol 3-kinase (PI3K) in the observed effect of aldosterone or hypotonic stress, we added 50 μM LY294002 (Sigma), a specific inhibitor of PI3K, to both sides of the cell monolayer.

Measurement of Transepithelial Electrical Conductance (G_t). G_t was measured with an EVOM ohmmeter (World Precision Instruments, Hertfordshire, U.K.) by using the intact epithelium cultured on filters of 23.1-mm diameter and with 4.19-cm^2 effective growth area of membrane (17). Changes in Na^+ permeability were determined as changes in the G_t across filters mounted in an Endohm 24 chamber (World Precision Instruments) from successive measurements of the transepithelial electrical resistance (TEER), as $G_t = 1/TEER$. G_t of whole monolayer was divided by the effective growth area of membrane and expressed per cm^2 of cells.

To determine whether any observed effect of aldosterone or hypotonic stress involved a direct or indirect action via Na^+ channels, we used 10 μM amiloride (Sigma) on the apical side of the cell monolayers.

ATP Release. Monolayers on the membrane filters were gently superfused with L-15 medium and equilibrated for 60 min in an Endohm 24 chamber, maintaining the apical and basolateral solution volumes at 2 ml. We quantified ATP release by using an ATP bioluminescent assay kit (Sigma) following a modified method previously reported (8). Briefly, a 500-μl sample was taken from the basolateral compartment and added in a mixture of 100 μl of luciferin/luciferase assay reagent and 500 μl of L-15 medium in a Petri dish. The dish was inserted into a light-tight compartment, and the ATP luminescence intensity was detected by an integrated photomultiplier-tube (814 Photomultiplier Detection System, Photon Technology International, West Sussex, U.K.). To account for constituents in the sample medium, which affect the sensitivity of the ATP assay, calibration curves were constructed by adding incremental concentrations of ATP standard to the same sample for each measured point in each series of studies.

ATPγS and Hexokinase. ATPγS (50 μM)(a nonhydrolyzable ATP analog) (Sigma) was added to the basolateral side of cell monolayer to assess the role of ATP on sodium reabsorption and cell morphology changes. To trap free ATP from the basolateral side, 6 units/ml hexokinase (Sigma) and 5 mM glucose (Sigma) was added to the basolateral compartment.

Results and Discussion

We have used SICM to image living A6 cells growing on filter supports in physiological conditions (11) to study the mechanism of aldosterone action. Fig. 1*B* presents a typical SICM topographical image of the apical membrane of A6 cells in a monolayer cultured on a membrane filter insert. For comparison, a scanning electron microscopy (SEM) image (Fig. 1*C*) of the same preparation reveals similar structures. Microvilli pro-

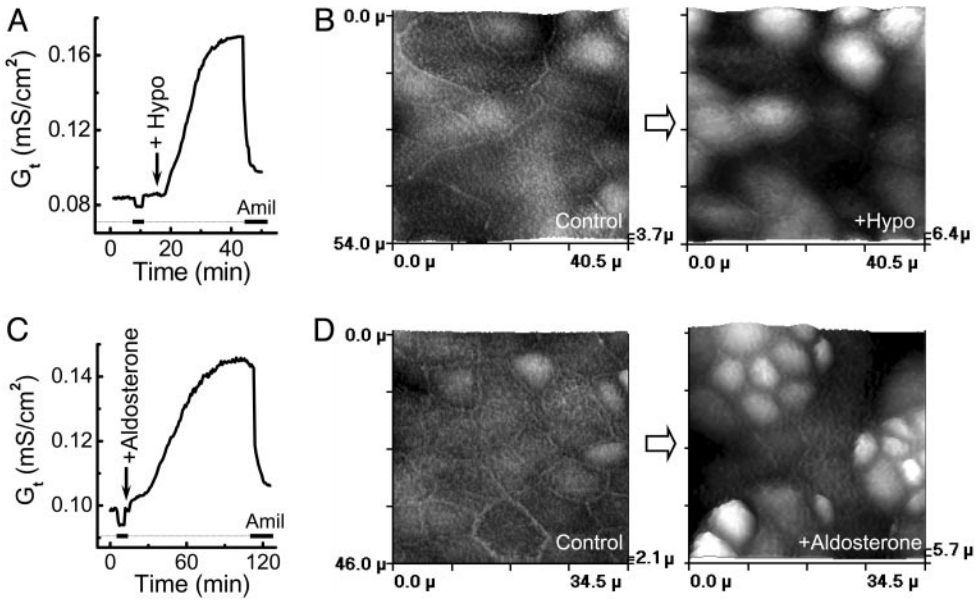

Fig. 2. Effect of osmotic stress and aldosterone on G_t and the topography of A6 cell monolayer. (*A*) Typical time-dependent effect of basolateral hypoosmotic stress on the amiloride-sensitive G_t^{ENaC} of A6 monolayer. (*B*) SICM images of a selected area of A6 monolayer cultured on a membrane filter scanned before (Control) and 1 h after basolateral hypotonic stress (+Hypo). (*C*) Typical time-dependent effect of aldosterone on the G_t of A6 monolayer. (*D*) SICM images of a selected area of A6 monolayer cultured on a membrane filter scanned before (Control) and 2 h after aldosterone stimulation (+Aldosterone).

jections and cell borders are clearly visible and comparable on both images.

The effects of localized basolateral hypoosmotic stress and aldosterone on sodium transport were studied. Fig. 2 *A* and *C* shows that both stimuli stimulated an increase in amiloride-sensitive sodium transport, with hypoosmotic stress producing a more marked activation than aldosterone. We then studied the effects of these two stimuli on cell morphology. The SICM images demonstrated that hypoosmotic stimulation resulted in prolonged cell morphology changes (Fig. 2*B*) that remained even after the regulatory volume decrease (RVD). These topographical changes with only a proportion of cells with apical membrane expansion are most likely the result of cell contraction. Previously, we have demonstrated that some A6 epithelial cells show slow lateral contraction under basal conditions (11). Fig. 2*D* shows typical topographical images of A6 cells before and after stimulation with aldosterone. Remarkably, aldosterone produced similar morphological changes as hypotonic stress, which occurred not in every cell, but rather in separate clusters of cells.

We next examined the relationship between cell contraction and sodium transport (Fig. 3). During aldosterone stimulation, successive 15-min scans of the same cells showed the contraction of individual cells (Fig. 3*A*, see cells marked 1, 2, and 3). The progressive recruitment of contracted cells in response to aldosterone or hypoosmotic stress (Fig. 3*B*) had a similar time course to that of the increase in amiloride-sensitive G_t (Fig. 2 *A* and *C*). However, the aldosterone-induced contraction was not blocked by amiloride but was blocked by 50 μM LY294002 (a specific PI3K inhibitor) (Fig. 3*B*).

To test whether cell contraction is directly associated with sodium transport, we individually studied noncontracted (Fig. 3*C Upper*) and contracted (Fig. 3*C Lower*) cells during aldosterone stimulation. The SICM images of noncontracted and contracted cells, along with cell-attach patch clamp single-channel recordings using our scanning patch clamp technique (14), are presented in Fig. 3 *C* and *D*. Epithelial sodium channel (ENaC) activity was found only in contracted cells (Fig. 3*D Lower*). Further high resolution SICM scans showed that contraction alters the cell membrane/cytoskeleton link with the loss of surface projection of microvilli (Fig. 3*E Lower*). Given the mechano-sensitivity of ENaC (10) and ENaC activity F-actin cytoskeleton dependency (18), these changes may result in the opening of the sodium channels (Fig. 3*F*). Moreover, LY294002, in addition to the cell contraction inhibition, also blocked the conductance changes induced by both aldosterone and hypotonic stress (data not shown).

However, it is unclear what causes cell contraction during hypoosmotic or aldosterone stimulation. A known modulator of epithelial cell contraction is purinergic stimulation that acts by means of intracellular Ca^{2+} elevation (19). As already discussed, others have demonstrated that hypotonic-induced sodium transport correlates with ATP release from epithelial cells into the basolateral compartment, and this acts via P2 receptors to stimulate a rise in intracellular Ca^{2+} (8). It is also well known that adenosine, as a product of the hydrolysis of extracellular ATP by ecto-nucleotidases via ADP and AMP, can increase the sodium transport in renal epithelia by the activation of P1 receptors (20). This finding, together with the wide distribution of purinergic receptors in the renal epithelia (21), suggests a possible common purinergic mechanism in ENaC activation by cell contraction.

To determine whether aldosterone, similar to hypotonicity, releases ATP from the basolateral side of A6 cells, we measured the change in transepithelial electrical conductance (G_t) (Fig. 4*A*) and the relationship of the rate of ATP release (R_{ATP}) (Fig. 4*B*) to amiloride-sensitive G_t^{ENaC}. Aldosterone increased amiloride-sensitive G_t^{ENaC} as expected, and this result was associated with a marked increase in ATP release.

To test whether ATP stimulation *per se* contracted epithelial cells, we imaged the response of A6 cell monolayer to basolaterally delivered ATPγS. Fig. 4*C* shows that ATP induced contraction in $\approx$75% of the monolayer cells.

The basolateral addition of nonhydrolyzable ATPγS produced an increase in amiloride-sensitive transepithelial conductance (Fig. 4*D*), which suggested that ATP release and G_t^{ENaC} were likely to be linked. We then added the ATP consumption system, hexokinase/glucose, to the basolateral compartment. Aldosterone had no effect on conductance in the absence of available extracellular ATP (Fig. 4*E*). When, however, hexokinase and

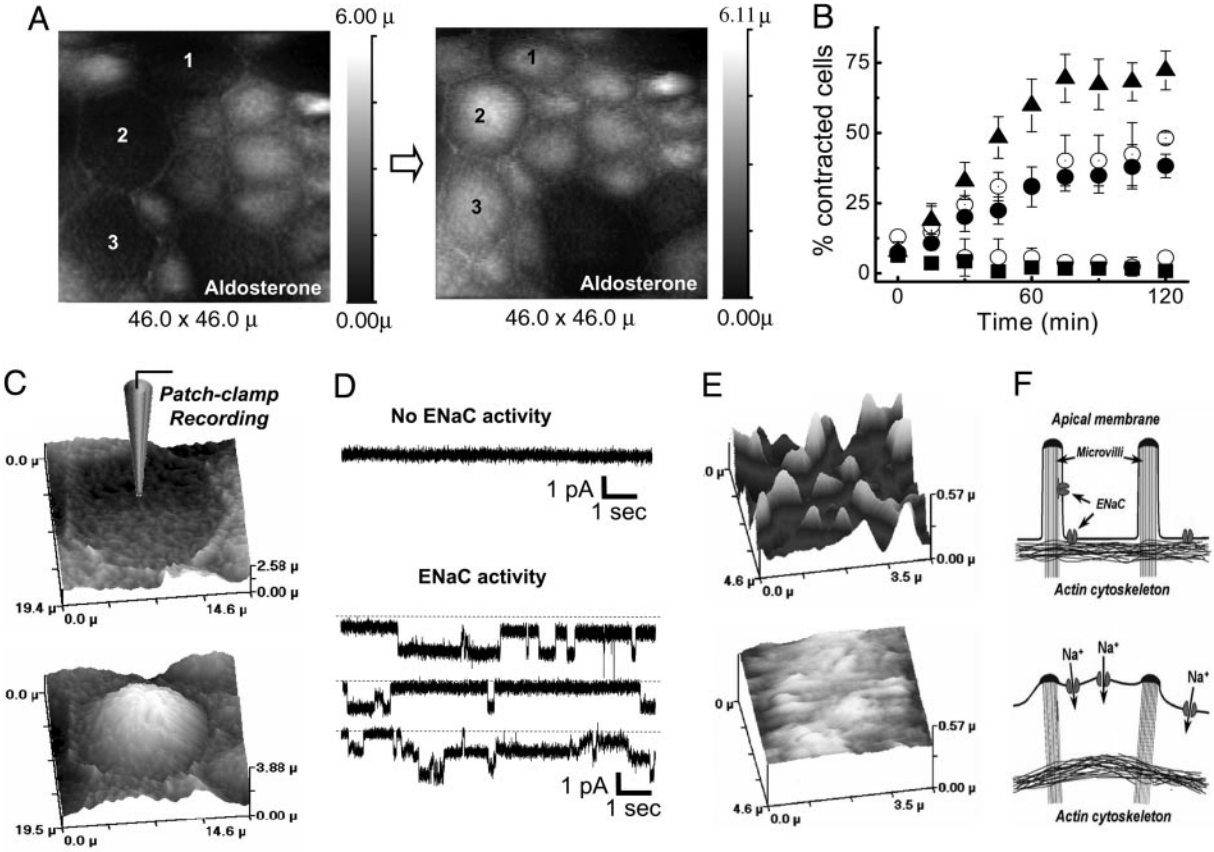

Fig. 3. Aldosterone induces cell contraction and sodium transport. (*A*) Topographical images of A6 cell monolayer, illustrating the cell contraction (observe cells 1, 2, and 3), obtained from two successive scans of continuous imaging separated by a 15-min interval during aldosterone stimulation. (*B*) Effect of aldosterone (●) ($n = 8$), aldosterone plus amiloride (⊙) ($n = 5$), aldosterone plus LY294002 (■) ($n = 7$), and hypoosmotic stress (▲) ($n = 7$) or without any stimulation (○) ($n = 8$) on the percentage of A6 cells contracted. All data were expressed as the mean values ± SE. (*C* and *D*) Smart patch clamp recordings of ENaC in the cell attach configuration from a contracted A6 cell (*Lower*) and noncontracted A6 cell (*Upper*), during aldosterone stimulation. The image at the left side of the recordings illustrates the morphology of the cell patched. (*E*) High-resolution SICM images showing the fine structure of the apical membrane of a contracted (*Lower*) and noncontracted (*Upper*) A6 cell during aldosterone stimulation. (*F*) Schematic model of aldosterone-induced cell contraction and ENaC activation. The apical membrane of the contracted A6 cell (*Lower*) lifts up, possibly activating the ENaCs. In the noncontracted cell (*Upper*), the typical microvilli structure of the apical membrane is maintained and there is no ENaC activation.

glucose were removed by washing the basolateral compartment, there was a rapid increase in G_t (Fig. 4*E*). In another complementary experiment, when hexokinase and glucose were added to an aldosterone-prestimulated A6 monolayer, the amiloride-sensitive G_t was reduced gradually (Fig. 4*F Upper* graph).

Knowing that ATP rapidly hydrolyzes to adenosine via ADP and AMP, we also checked the sodium transport effect of ADP and adenosine. ADP had no effect on conductance in contrast with the expected increase with adenosine (20) (data not shown). DPCPX (100 nM) (8-cyclopentyl-1,3-dipropyl-xanthine), a P1 receptor antagonist, added to the basolateral side of the cell monolayer, reduced the aldosterone-stimulated sodium transport (Fig. 4*F Lower* graph). Suramin (100 μM) and/or pyridoxal phosphate-6-azo(benzene-2,4-disulfonic acid) (PPADS) (P2 receptor blockers) not only did not reduce the Na^+ conductance, but suramin markedly increased it (data not shown).

Using these results, we propose an alternative model of aldosterone-induced epithelial sodium transport (Fig. 5). Aldosterone enters the cell and, by mechanisms yet to be determined, stimulates ATP release. ATP is then excreted from the cell and, as has been demonstrated in many cell types, signals via an autocrine/paracrine system via P2 purinergic receptors (9). Excreted ATP rapidly hydrolyzes to ADP, AMP, and adenosine. Adenosine being also a purinergic stimulator acts via its own P1 receptors. Our experiments demonstrate that both aldosterone and hypotonic stress induced Na^+ transport and that cell contraction can be blocked by LY294002, indicating the importance of the PI3K pathway in ENaC activation. Many studies confirm that both ATP and adenosine increase intracellular calcium (8, 20). Macala and Hayslett (20) suggested that renal sodium transport might be controlled by locally produced adenosine acting as an autacoid, and therefore induces a local physiological effect (20). We postulate that this purinergic activation produces the cell contraction that we have observed. A similar mechanism has been reported in myoepithelial cells (19). The contraction profoundly alters the apical membrane topography with the loss of normal microvillar architecture. Given the mechanosensitivity of ENaC (10) and ENaC activity F-actin cytoskeleton dependency (18), these changes may also facilitate the opening of the sodium channels (Fig. 5).

In renal epithelial cells, ATP is released from the cell in a polarized manner, either at the apical or basolateral cell surfaces, for the purpose of autocrine and paracrine regulation of the epithelial function (21, 22). It is important to recognize the very different effects of ATP when released into the basolateral as compared with the apical compartment. Thus, *in vivo* stimulation experiments of apical P2 receptors inhibits sodium reabsorption in collecting ducts, but the identity of the receptor subtype(s) involved remains elusive (23).

Traditionally, the effect of aldosterone is divided into an early response (0.5–3 h), with a 2- to 3-fold increase in sodium

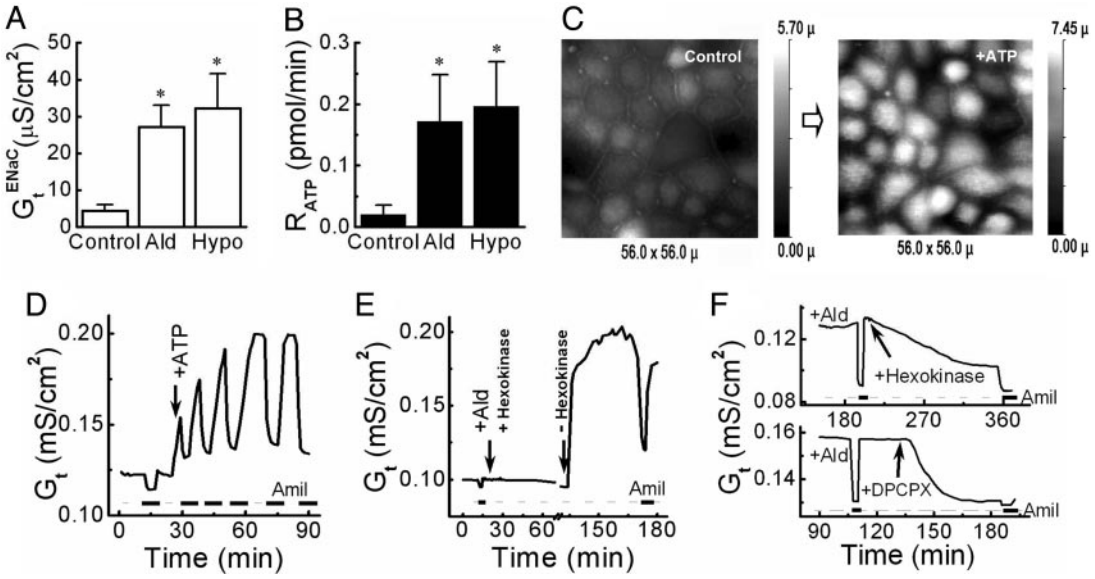

Fig. 4. Aldosterone induces ATP release and changes the morphology of A6 cells. (*A*) Effect of control ($n = 8$), aldosterone ($n = 8$), and basolateral hypotonic stress ($n = 7$) on the amiloride-sensitive transepithelial electrical conductance (G_t^{ENaC}) of A6 cell monolayer. (*B*) Rate of ATP release (R_{ATP}) from A6 cell monolayers during control ($n = 7$), aldosterone stimulation ($n = 7$), and basolateral hypotonic stress ($n = 5$). All data in *A* and *B* were expressed as the average of experiments (mean ± SE.). Asterisk denotes value statistically different from the control based on Student's *t* test (*, $P < 0.05$). (*C*) Effect of basolateral ATPγS on the topography of A6 cells. Shown are two SICM topographical images of a selected area of a living A6 cell monolayer before (Control) and after (+ATP) stimulation with ATPγS. (*D*) Effect of ATPγS on G_t of A6 cell monolayer. ATPγS (50 μM) was added to basolateral side. (*E*) Effect of hexokinase on the aldosterone-induced G_t of A6 cell monolayer. Aldosterone and hexokinase/glucose were added together to the basolateral compartment at the time marked by the arrow, and then the hexokinase/glucose was removed 90 min later. (*F*) Hexokinase and glucose were added to the basolateral compartment of an aldosterone-stimulated A6 cell monolayer at the time marked by the arrow (*Upper*). DPCPX (100 nM), a P1 receptor antagonist, was added to the basolateral compartment of an aldosterone-stimulated A6 cell monolayer at the time marked by the arrow (*Lower*). The thick lines on the bottom of *D*, *E*, and *F* indicate the application of amiloride to the apical side of the A6 cell monolayer.

reabsorption, and a later phase (3–24 h), where the increase is up to 20-fold (24). Although the later stages are well studied, the dominant early effect of modulating ENaC activity before any increase in ENaC subunit mRNA or protein is poorly understood (25). There are two potential ways to increase sodium transport: augmenting the number of cell membrane channels, or enhancing the open probability of the existing ENaCs. Some studies suggest that aldosterone does not regulate the sodium channel pool in the early stages (26). Others conclude that the effect is due exclusively to an increase in channel density (27), and that aldosterone, vasopressin, and insulin act on sodium transport by promoting the incorporation of channels in the apical membrane (28). Conversely, several groups have suggested that aldosterone increases the ENaC open probability (15), possibly by posttranslational modification (26, 29). It has been suggested that regulation of trafficking and/or functioning of sodium channels is controlled by aldosterone-induced modulatory proteins and kinases (30). One regulatory cascade proposed acts via aldosterone-induced expression of small G protein K-Ras2A, with subsequent activation of PI3K, which produces phosphoinositol-3,4,5-trisphosphate (PIP_3) and that this is a direct regulator of ENaC open probability (29). This regulation also involves serum- and glucocorticoid-kinase (SGK1) that prevents ENaC degradation and mitogen-activated protein kinase (MAPK) that in contrast stimulates channel degradation (31, 32). In A6 cells, hypotonicity, as well as aldosterone, induces

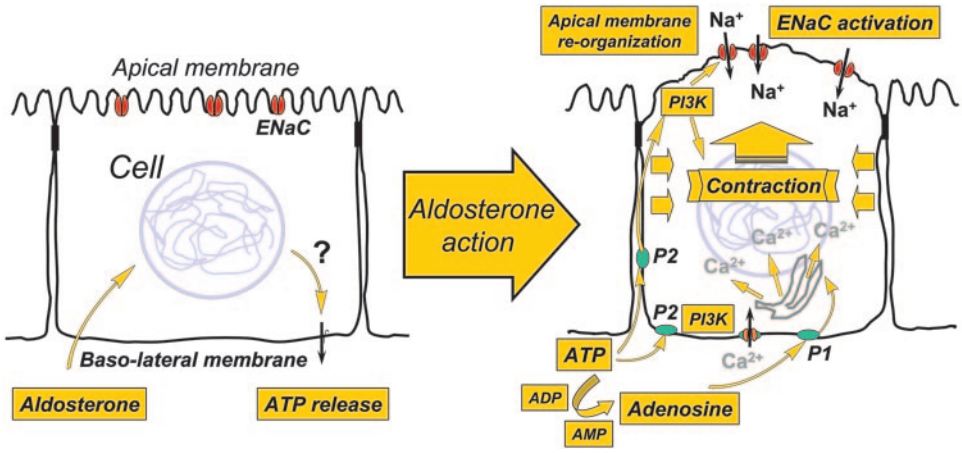

Fig. 5. A model of aldosterone stimulation of sodium transport and cell contraction in epithelial cells.

SGK1 expression (7). However, studies in the SGK1 knockout mouse demonstrated that renal salt handling is normal when the animals are on a standard salt intake but impaired with dietary salt restriction, suggesting that SGK1 participates in, but does not fully account for, mineralocorticoid regulation of sodium reabsorption (33).

Our results may well explain the controversy in the literature concerning the early phase of aldosterone action. ATP produces rapid contraction of individual cells, and these cells demonstrate channel activity. Thus, aldosterone acting via ATP would seem to increase the open probability of ENaC. However, with time there is progressive recruitment of individual cells that parallels the slow increase in electrical conductance. This incremental change in the number of transporting cells would be interpreted as a progressive increase in the apparent apical membrane channel density.

The evolutionary aspects of this system are likely to be important. The transition of the protovertebrates from salt to fresh water required the development of a system that could regulate ion transport so as to maintain the internal milieu in the face of a very variable external environment. In this context, it is of interest that P2X receptors are apparently restricted to vertebrates (34). During evolution, aldosterone seems to have adopted the same mechanism of action that the cell uses to regulate cell volume in response to a change in osmolality. Hypotonicity is a potent stimulus for ATP release across the renal epithelia (8). We have demonstrated that the application of a hypoosmolar stimulus to the basolateral side of the A6 monolayer produces a pattern of cell contraction that is very similar to that produced by either aldosterone or ATP. Many studies have confirmed that ATP release is concerned with the control of cell volume (35).

The regulation of extracellular fluid volume and sodium balance are key determinants of blood pressure. In about one third of patients with so-called essential hypertension, plasma renin activity is low in association with normal aldosterone levels. The reason for this relationship is unknown. One possibility is that, in some individuals, there may be a greater response of the renal epithelial cells to aldosterone, leading to enhanced sodium reabsorption. It is interesting to speculate in relation to our results that there could well be important variations in this purinergic control system, some of which might underlie this and other conditions. It would seem likely that a number of stimuli of sodium transport may also have adopted this very basic cell control and energy system. As Sir Peter Medawar used to say: "It is not molecules which evolved, but simply the use to which they are put."

These results suggest that there is a very real need to return to the fundamental studies carried out by Izzy Edelman and his colleagues nearly 40 years ago and determine the mechanism by which aldosterone increases ATP production (36).

This paper is dedicated to the memory of Professor Isidore S. "Izzy" Edelman, member of the National Academy of Sciences, who died in 2004. This work was supported by the Wellcome Trust and the Biotechnology and Biological Sciences Research Council.

1. Simpson, S. A., Tait, J. F., Wettstein, A., Neher, R., von Euw, J., Schindler, O. & Reichstein, T. (1954) *Experientia* **10,** 132–133.
2. Edelman, I. S. & Fimognari, G. M. (1968) *Recent Prog. Horm. Res.* **24,** 1–44.
3. Ussing, H. H. & Zerahn, K. (1951) *Acta Physiol. Scand.* **23,** 110–127.
4. Crabbé, J. (1961) *J. Clin. Invest.* **40,** 2103–2110.
5. Crabbé, J. (1963) *Nature* **200,** 787–788.
6. Edelman, I. S., Bogoroch, R. & Porter, G. A. (1963) *Proc. Natl. Acad. Sci. USA* **50,** 1169–1177.
7. Rozansky, D. J., Wang, J., Doan, N., Purdy, T., Faulk, T., Bhargava, A., Dawson, K. & Pearce, D. (2002) *Am. J Physiol. Renal Physiol.* **283,** F105–F113.
8. Jans, D., Srinivas, S. P., Waelkens, E., Segal, A., Lariviere, E., Simaels, J. & Van Driessche, W. (2002) *J. Physiol. (London)* **545,** 543–555.
9. Burnstock, G. & Williams, M. (2000) *J. Pharmacol. Exp. Ther.* **295,** 862–869.
10. Awayda, M. S. & Subramanyam, M. (1998) *J. Gen. Physiol.* **112,** 97–111.
11. Gorelik, J., Zhang, Y., Shevchuk, A. I., Frolenkov, G. I., Sanchez, D., Lab, M. J., Vodyanoy, I., Edwards, C. R., Klenerman, D. & Korchev, Y. E. (2004) *Mol. Cell. Endocrinol.* **217,** 101–108.
12. Korchev, Y. E., Milovanovic, M., Bashford, C. L., Bennett, D. C., Sviderskaya, E. V., Vodyanoy, I. & Lab, M. J. (1997) *J. Microsc. (Oxford)* **188,** 17–23.
13. Gorelik, J., Gu, Y., Spohr, H. A., Shevchuk, A. I., Lab, M. J., Harding, S. E., Edwards, C. R., Whitaker, M., Moss, G. W., Benton, D. C., *et al.* (2002) *Biophys. J.* **83,** 3296–3303.
14. Gu, Y., Gorelik, J., Spohr, H. A., Shevchuk, A., Lab, M. J., Harding, S. E., Vodyanoy, I., Klenerman, D. & Korchev, Y. E. (2002) *FASEB J.* **16,** 748–750.
15. Kemendy, A. E., Kleyman, T. R. & Eaton, D. C. (1992) *Am. J. Physiol.* **263,** C825–C837.
16. Hansma, P. K., Drake, B., Marti, O., Gould, S. A. & Prater, C. B. (1989) *Science* **243,** 641–643.
17. Zettl, K. S., Sjaastad, M. D., Riskin, P. M., Parry, G., Machen, T. E. & Firestone, G. L. (1992) *Proc. Natl. Acad. Sci. USA* **89,** 9069–9073.
18. Cantiello, H. F., Stow, J. L., Prat, A. G. & Ausiello, D. A. (1991) *Am. J Physiol.* **261,** C882–C888.
19. Nakano, H., Furuya, K., Furuya, S. & Yamagishi, S. (1997) *Pflügers Arch.* **435,** 1–8.
20. Macala, L. J. & Hayslett, J. P. (2002) *Am. J. Physiol. Renal Physiol.* **283,** F1216–F1225.
21. Schwiebert, E. M. & Kishore, B. K. (2001) *Am. J. Physiol. Renal Physiol.* **280,** F945–F963.
22. Schwiebert, E. M. & Zsembery, A. (2003) *Biochim. Biophys. Acta* **1615,** 7–32.
23. Shirley, D. G., Bailey, M. A. & Unwin, R. J. (2005) *Am. J Physiol. Renal Physiol.* **288,** F1243–F1248.
24. Alvarez de la Rosa, D., Canessa, C. M., Fyfe, G. K. & Zhang, P. (2000) *Annu. Rev. Physiol.* **62,** 573–594.
25. Chen, S. Y., Bhargava, A., Mastroberardino, L., Meijer, O. C., Wang, J., Buse, P., Firestone, G. L., Verrey, F. & Pearce, D. (1999) *Proc. Natl. Acad. Sci. USA* **96,** 2514–2519.
26. Kleyman, T. R., Coupaye-Gerard, B. & Ernst, S. A. (1992) *J. Biol. Chem.* **267,** 9622–9628.
27. Helman, S. I., Liu, X., Baldwin, K., Blazer-Yost, B. L. & Els, W. J. (1998) *Am. J. Physiol.* **274,** C947–C957.
28. Alvarez de la Rosa, D. & Canessa, C. M. (2003) *Am. J. Physiol. Cell Physiol.* **284,** C404–C414.
29. Eaton, D. C., Malik, B., Saxena, N. C., Al Khalili, O. K. & Yue, G. (2001) *J. Membr. Biol.* **184,** 313–319.
30. Snyder, P. M. (2002) *Endocr. Rev.* **23,** 258–275.
31. Pearce, D., Verrey, F., Chen, S. Y., Mastroberardino, L., Meijer, O. C., Wang, J. & Bhargava, A. (2000) *Kidney Int.* **57,** 1283–1289.
32. Tong, Q., Booth, R. E., Worrell, R. T. & Stockand, J. D. (2004) *Am. J. Physiol. Renal Physiol.* **286,** F1232–F1238.
33. Wulff, P., Vallon, V., Huang, D. Y., Volkl, H., Yu, F., Richter, K., Jansen, M., Schlunz, M., Klingel, K., Loffing, J., *et al.* (2002) *J. Clin. Invest.* **110,** 1263–1268.
34. North, R. A. (2002) *Physiol. Rev.* **82,** 1013–1067.
35. Wang, Y., Roman, R., Lidofsky, S. D. & Fitz, J. G. (1996) *Proc. Natl. Acad. Sci. USA* **93,** 12020–12025.
36. Fimognari, G. M., Fanestil, D. D. & Edelman, I. S. (1967) *Am. J. Physiol.* **213,** 954–962.